Influence of Particle Distribution on Macroscopic Properties of Particle Flow Model

Bin Gou
SWJTU: Southwest Jiaotong University
Mengqi Zhang (mzhang@swjtu.edu.cn)
SWJTU: Southwest Jiaotong University
Jiliang Mo
SWJTU: Southwest Jiaotong University

Research Article

Keywords: Numerical modelling, Particle distribution, Statistical analysis, Normality test, Minimum sample size

Posted Date: June 9th, 2021

DOI: https://doi.org/10.21203/rs.3.rs-576711/v1

Influence of Particle Distribution on Macroscopic Properties of Particle Flow Model

Bin Gou[1], Mengqi Zhang[1*], Jiliang Mo[1]

1. Tribological Design Laboratory of Shield/TBM Equipment, Southwest Jiaotong University, Chengdu 610031, China

Abstract

The particle flow discrete element models for uniaxial compression and tensile tests of rocks are established to study the influence of the particle distribution randomness on the macroscopic mechanical properties of such model. The results of macroscopic mechanical properties show strong discreteness due to the variance of particle distributions, in which compressive strength, tensile strength and Poisson's ratio follow the normal distribution and the Young's modulus follows the negative skewness distribution. The average values of the macroscopic strength obtained based on multiple calculations with different particle distributions should be used for the calibration of microscopic parameters. According to the relationship between sample size and deviation of macro strength averages, the minimum calculation number required to obtain high-precision macro strength with different confidence levels is given.

Key words: Numerical modelling; Particle distribution; Statistical analysis; Normality test; Minimum sample size

NOTATION

g_1 is the skewness of a statistic

g_2	is the kurtosis of a statistic
υ_i	is the *i*-order center distance of a statistic
E(X)	is the expectation of a statistic
X-E(X)	is the deviation of a statistic
Var(X)	is the variance of a statistic
n	is the size of a statistic
x_j	is the j^{th} order statistic
$\overline{x}$	is the mean of a statistic
u_i	is the U test coefficient for skewness ($i=1$) or kurtosis ($i=2$)
σ_{gi}	is standard error of skewness ($i=1$) or kurtosis ($i=2$)
α	is the specified significance level
$u_{\frac{\alpha}{2}}$	is the U statistic for bilateral tests at the specified significance level
D	is the normal statistic for the LL test
$F^*(X)$	is the cumulative normal distribution function of a statistic
$S_n(X)$	is the cumulative distribution function of a statistic
W	is the normal statistic for the S-W test
x_i	is the i^{th} variable values of a statistic
V	is the covariance matrix of the variable
m_i	is the expected value of *i* order statistic sampled from the standard normal distribution of the random variable
P	is the significance level corresponding to the statistics when the variable are

	tested by LL and S-W
CL	is the specified confidence level
μ	is the sample mean
δ	is the sample variance
n_{min}	is the minimum sample size
Z	is the value corresponding to the confidence specified in the normal probability distribution table
S	is the standard deviation of the population sample
$\Delta_{\bar{x}}$	is the allowable error

1

1 Introduction

The basic principle of the particle flow discrete element method is to use the collection of particles to simulate the rock and soil, and to duplicate the macroscopic mechanical behavior of such materials through the interaction between particles. It is one of the most popular methods to study the problem of rock and soil mechanics(Hrd *et al*., 2000; Cook *et al*., 2004; Onate *et al*., 2004; McDowell *et al.*, 2006; Qin *et al*., 2013; Zhang *et al*., 2015; Zhao *et al*., 2019; Xie *et al*., 2020). The microscopic parameters of particle flow models are usually not directly equal to the macroscopic mechanical parameters of materials. Simulations of strength tests (uniaxial, biaxial, Brazilian splitting experiments, etc.) are needed to establish the relationship between model microcosmic parameters and the macroscopic mechanical properties of rocks, such a process is called calibration (Xia *et al*., 2018; Shi *et al.*, 2019). The particle distribution may have a significant influence on the macroscopic mechanical properties of the model because the change of particle locations will affect the crack initiation and propagation in the rock model. Therefore, a one-time simulation under a given particle distribution may not be able to obtain the accurate relationship between microscopic parameters and macroscopic strength in calibrations. This paper studies the influence of the randomness of particle distribution on the macroscopic mechanical parameters of the discrete element model, to improve the calibration accuracy of the particle flow discrete element model.

Scholars have studied the factors that affect the macroscopic properties. Potyondy *et al*. (Potyondy *et al*., 2004) found that Young's modulus and tensile strength are strongly correlated

with particle size. Yoon, Wang, Castro-Filgueira, Boutt and Martin et al. (Boutt *et al*., 2002; Cho *et al*., 2007; Yoon *et al*., 2007; Wang *et al*., 2010; Castro-Filgueira *et al.*, 2017) pointed out that the effective stiffness and stiffness ratio of intergranular contact have the greatest effect on Young's modulus, and the relationship between effective contact modulus and Young's modulus is linear. Tangential and normal contact strength have the greatest influence on compressive strength and tensile strength, and the relationship between contact strength and compressive strength is linear. The stiffness ratio has the greatest influence on Poisson's ratio, but only has minor influence on other macro parameters. The particle friction coefficient merely affects the post-peak response of the particle flow model. Wang and Martin et al. (Wang, 1981); Schöpfer *et al*., 2009) found that Young's modulus, uniaxial compressive strength (UCS), tensile strength (T), strength ratio (UCS/T) and internal friction angle would all decrease with the increase of porosity, while porosity had almost no influence on Poisson's ratio. Castro-Filgueira et al. (Castro-Filgueira *et al.*, 2016)studied confining pressure and found that Young's modulus, compressive strength and tensile strength all increased with the increase of confining pressure, but had little impact on Poisson's ratio. Coetzee et al. (Coetzee *et al.*, 2009) showed that the internal friction angle increased with the increase of particle stiffness and friction coefficient, while the friction coefficient had little influence on the system stiffness.

The above researches have made a lot of achievements in the aspects of model calibration. However, there are still some unsolved problems. The heterogeneity and randomness of natural rocks lead to a significant discreteness of macroscopic mechanical parameters of such material

(Yamaguchi, 1970; Ruffolo *et al*, 2009; Cui *et al.*, 2017). For the discrete element model, the randomly distributed particles could be used to simulate the heterogeneous characteristic of rocks, but how does particle distribution affect the macroscopic strength of the model has not been systematically studied yet. In addition, the particle distributions are usually different in the model for calibration and that for solving practical problems. The difference of particle distributions changes the crack initiation location and propagation path, which may have a significant influence on the macroscopic mechanical properties of the model. That is, due to the randomness of particle distribution, two models with the identical microscopic parameters may not provide the same macroscopic strength. The calibration according to only one calculation without the consideration of particle distribution may not correctly reveal the relation between microscopic parameters and macroscopic strength. Therefore, it is necessary to study the coupling effect of the particle distribution and microscopic parameters on the macroscopic strength of the model, and then to propose a statistic-based calibration principle using the average values from multiple calculations.

In this paper, the particle flow discrete element models for simulating uniaxial compression and tensile tests of rocks are established. Based on a large number of numerical simulations, the relationship between the particle distribution randomness and the macroscopic mechanical response of the model is obtained by using statistical analysis methods. And the minimum sample size required to provide high-precision averages of macroscopic mechanical properties are obtained. The applicability of the "three in five tests for the mean" method

(calculate five times with different particle distribution, and obtain the average value after removing the maximum and minimum) for calibration is verified.

2 Modeling of uniaxial tests for rocks

Natural rocks are characterized by discontinuity, anisotropy, heterogeneity, inelasticity and other inherent characteristics (Jing, 2003). Therefore, for rock modeling the continuum hypothesis may no longer applicable. The particle flow discrete element method is a novel discontinuous medium method, which uses a series of discrete disk (2D) or spherical (3D) particles to model the rock, and to reflects the deformation and failure of rock by the relative position, motion state and bond relationship of the particles. Particle flow discrete element method has unique advantages in simulating large deformation and brittle failure of rocks under various external forces (Mehranpour *et al*, 2017; Castro-Filgueira *et al*, 2020; Tian *et al.*, 2020)

The Idaho basalt reported in the reference (Moon *et al*, 2012) is selected as the representative of rocks in this paper. The macroscopic properties of Idaho basalt are: Young's modulus 9.66 GPa, Poisson's ratio 0.21, compressive strength 28.4 MPa, and tensile strength 6.6 MPa. The two-dimensional simulations of uniaxial compression and uniaxial tensile tests are used for the calibration, as shown in Fig. 1 (a) and (c). The height and width of the models are 100 mm and 50 mm, respectively. Rigid walls are located on the upper and lower sides of the sample for axial loading. The crack distributions inside the rock samples under uniaxial compression and uniaxial tensile load are shown in Fig. 1 (b) and (d), respectively. The microscopic parameters are calibrated according to the traditional method (Castro-Filgueira *et al.*, 2017) without

changing particle distribution yet, to obtained the benchmark for the subsequent study. The macroscopic mechanical properties of the model after calibration are shown in Table 1 and the corresponding microscopic parameters are shown in Table 2.

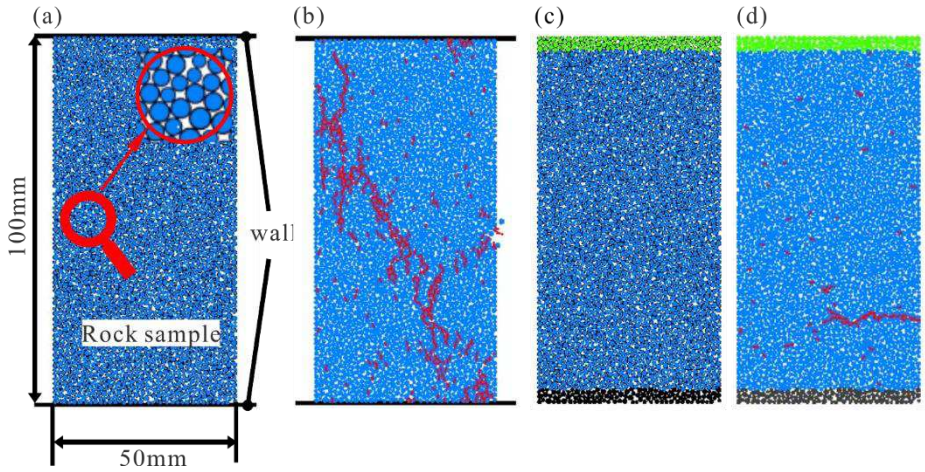

Fig. 1 Particle flow models for simulating uniaxial tests and typical results: (a) model for uniaxial compression tests; (b) crack distribution after uniaxial compression tests; (c) model for uniaxial tensile tests; (d) crack distribution after uniaxial tensile tests

Table 1 Macroscopic mechanical properties of particle flow model after calibration

Items	Values		Deviation
	Model	Experiment (Moon and Oh, 2012)	
Young's modulus	9.5 GPa	9.66 GPa	1.66%
Compressive strength	28.63 MPa	28.4 MPa	0.81%
Tensile strength	6.49 MPa	6.6 MPa	1.67%
Poisson's ratio	0.211	0.21	0.48%

Table 2 Micromechanical parameters of particle flow model after calibration

Categories	Items	Symbols	Values
General	Lower limit of particle diameter, mm	cm_Dlo	2

	Upper limit of particle diameter, mm	cm_Dup	1.66
	Particle density, kg/m^3	cm_densityVal	2650
	Damping coefficient	cm_localDampFac	0.7
Linear contact	Effective modulus, GPa	pbm_emod	6.28
	Friction coefficient	pbm_fric	0.50
	Stiffness ratio	pbm_krat	1.45
Parallel bond	Initial gap tolerance, mm	pbm_igap	0.1
	Radius multiplier	pbm_rmul	1.00
	Effective modulus, GPa	pbm_bemod	6.28
	Stiffness ratio	pbm_bkrat	1.45
	Moment contribution factor	pbm_mcf	1.00
	Average of tensile strength, MPa	pbm_ten_m	16.5
	Standard deviation of tensile strength, MPa	pbm_ten_sd	4.125
	Average of cohesion, MPa	pbm_coh_m	16
	Standard deviation of cohesion, MPa	pbm_coh_sd	4
	Frictional angle, degree	pbm_fa	30.00

To illustrate the influence of particle distributions on the macroscopic mechanical parameters of the model, ten simulations of uniaxial compression and tensile tests with different particle distributions (all other parameters maintain constant) are performed and the corresponding stress-strain curves are shown in Fig. 2. The results show significant discreteness, where the maximum difference of the simulated compressive strength is over 10 MPa, accounting for 30% of the experimental measured value. The tensile strength is also strongly affected by the randomness of particle distributions; the maximum difference of simulated tensile strength in Fig. 2(b) is more than 4.5 MPa, accounting for about 70% of the experimental measured value. The above-mentioned results illustrate the necessity of a systematically investigation on the statistical rule of the particle distribution effect on the macroscopic mechanical properties of the particle flow discrete element model.

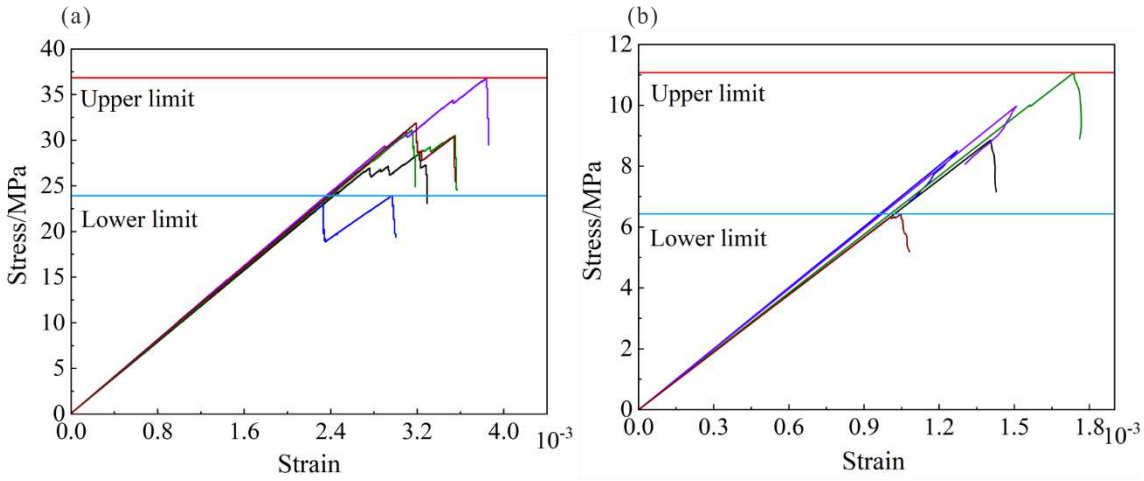

Fig. 2 Stress-strain response: (a) uniaxial compression tests; (b) uniaxial tensile tests

3 Statistical analysis on the results of macroscopic mechanical properties

The results of 500 simulations of rock compression and tensile tests with different particle distribution are collected as the sample base for the following statistical analysis: 1) Conducting normality test to obtain the probability distributions of the simulation results. 2) Determining the minimum sample size that could produce high-precision average values of macroscopic mechanical properties. 3) Examining the precision of average values obtained from the commonly used "three in five tests for the mean" method to verify the applicability of such method in the calibration of particle flow model.

3.1 Normality test

The normality test is commonly used to determine whether a sample follows the normal distribution. The popular normality test methods including skewness and kurtosis coefficient test (U test), Lilliefors test (LL), Shapiro-Wilk test (S-W) and Kolmogorov-Smirnov test (K-S), as well as graphic methods such as Q-Q graph, P-P graph and histogram (Keskin *et al.*,

2006; Mohd *et al.*, 2011; Yap *et al.*, 2011; Lee *et al.*, 2016).The applicable scope of the above-mentioned normality test methods has not been clearly defined at present. Taking the S-W method as an example, the references (Mohd *et al*, 2011) point out that the S-W test is applicable to the case with a sample size greater than 100, while the researcher (Society,R.S, 2019) insists that the S-W test is suitable for data with a sample size of 3~2000, and there are also literatures believe that the S-W test is the most accurate approach for any sample size (Mohd *et al*, 2011; Society,R.S, 2019). Therefore, to ensure the correctness of normal test results, this work comprehensively uses a variety of normality test methods, including the U test, LL test and S-W test, and supplemented by histogram and Q-Q graph.

The parameters required for the normality tests are shown below.

1) Skewness and kurtosis coefficient test

Skewness is a parameter that reflects the degree and direction of data distribution skewed, which is defined as (Keskin, 2006; (Trust, 2016):

$$g_1 = \frac{\upsilon_3}{\upsilon_2^{3/2}} = \frac{E[X - E(X)]^3}{[Var(X)]^{3/2}}$$

1.

$$\upsilon_i = \frac{1}{n-1}\sum_{j=1}^{n}(x_j - \bar{x})^i$$

2.

Kurtosis is a parameter that represents the peak value of the probability density

147 distribution curve at the mean, which is defined as (Keskin, 2006; Trust, 2016):

148 $$g_2 = \frac{\upsilon_4}{\upsilon_2^{\ 2}} - 3 = \frac{E[X - E(X)]^4}{[Var(X)]^2} - 3$$

149 3.

150

151 The corresponding U test value is calculated as:

152 $$u_i = \frac{g_i}{\sigma_{gi}} (i = 1, 2)$$

153 4.

154

155 The variable rejects the normal distribution hypothesis when $|u_i| > u_{\frac{\alpha}{2}}$.

156

157 2) LL test

158 The key parameter *D* of LL test is defined as (Yap *et al*, 2011; Mohd *et al* , 2011):

159 $$D = max\left|F^*(X) - S_n(X)\right|$$

160 5.

161

162 When $D > D(n,\alpha)$ (Massey, 1951) ($D(n,\alpha)$ is the statistical threshold of LL test at the

163 specified significance level α and sample size *n*; for the same sample size, it decreases with

164 increasing confidence level) the variable rejects the normal distribution hypothesis.

165

166 3) S-W test

The S-W test is the first normal test method that can be used to detect deviations in skewness, kurtosis, or both exist deviation. The key parameters of S-W test is defined as (Shapiro and Wilk, 1965, 1972; Keskin, 2006; Öztuna, Elhan and Tüccar, 2006; Mohd Razali and Bee Wah, 2011; Yap and Sim, 2011):

$$W = \frac{\left(\sum_{i=1}^{n} a_i x_i\right)^2}{\sum_{i=1}^{n}\left(x_i - \bar{x}\right)^2} \tag{6}$$

$$a_i = \left(a_1, \ldots, a_n\right) = \frac{m^T V^{-1}}{\sqrt{\left(m^T V^{-1} V^{-1} m\right)}} \tag{7}$$

$$m = \left(m_1, \ldots, m_n\right)^T \tag{8}$$

When $W < W(n,\alpha)$ ($W(n,\alpha)$ is the statistical threshold of S-W test at the specified significance level α and sample size n, it increases with significance level for the same sample size) the variable X rejects the normal distribution hypothesis.

The above-mentioned methods are applied to implement the normality tests for the simulated macroscopic property results of rock models with different particle distributions. The confidence coefficient is set to be 95% (i.e. confidence level CL=0.95, significance level α=0.05), and the results of normality test are shown in Table 3. The skewness U test value u_1

of the Young's modulus is -4.45, which are without the range of -1.96~1.96 (α=0.05 look-up the normal distribution table has $u_{\frac{\alpha}{2}}=1.96$); and the significance level P (P is the significance level corresponding to the statistics when the variable are tested by LL and S-W) of both the LL test and the S-W test is 0.015 and 0, respectively, which is less than the corresponding confidence standard α=0.05. It can be seen from Fig. 3 (a) and Fig. 4 (a) that the frequency distribution histogram is in poor agreement with the normal distribution curve, a large number of data points are outside the standard range corresponding to the confidence level of the Q-Q graph. To sum up, Young's modulus do not obey normal distribution.

According to Table 3, Fig. 3 and Fig. 4, all normal test statistics of compressive strength, tensile strength and Poisson's ratio are within the standard range corresponding to the confidence level. And the frequency distribution histogram is in good agreement with the normal distribution curve, and few data points in the Q-Q diagram are beyond the standard range of confidence levels. In conclusion, compressive strength, tensile strength and Poisson's ratio obey normal distribution.

Table 3 Normal test of stochastic simulation results of particle distribution

Items	Young's modulus	Compressive strength	Tensile strength	Poisson's ratio
Mean	9.39	28.26	6.82	0.184
Std. Deviation	0.435	2.51	0.583	0.009
Skewness, g_1	-0.636	-0.12	0.055	0.07
Skewness Std. Deviation, σ_{g1}	0.143	0.143	0.143	0.143
U test, u_1	-4.45	-0.84	0.38	0.49
Kurtosis, g_2	0.494	-0.42	-0.066	0.066

Kurtosis Std. Deviation, σ_{g2}	0.286	0.286	0.286	0.286
U test, u_2	1.73	-1.47	-0.23	0.23
LL (P)	0.015	0.2	0.063	0.2
S-W (P)	0	0.172	0.812	0.876
Normality	No	Yes	Yes	Yes

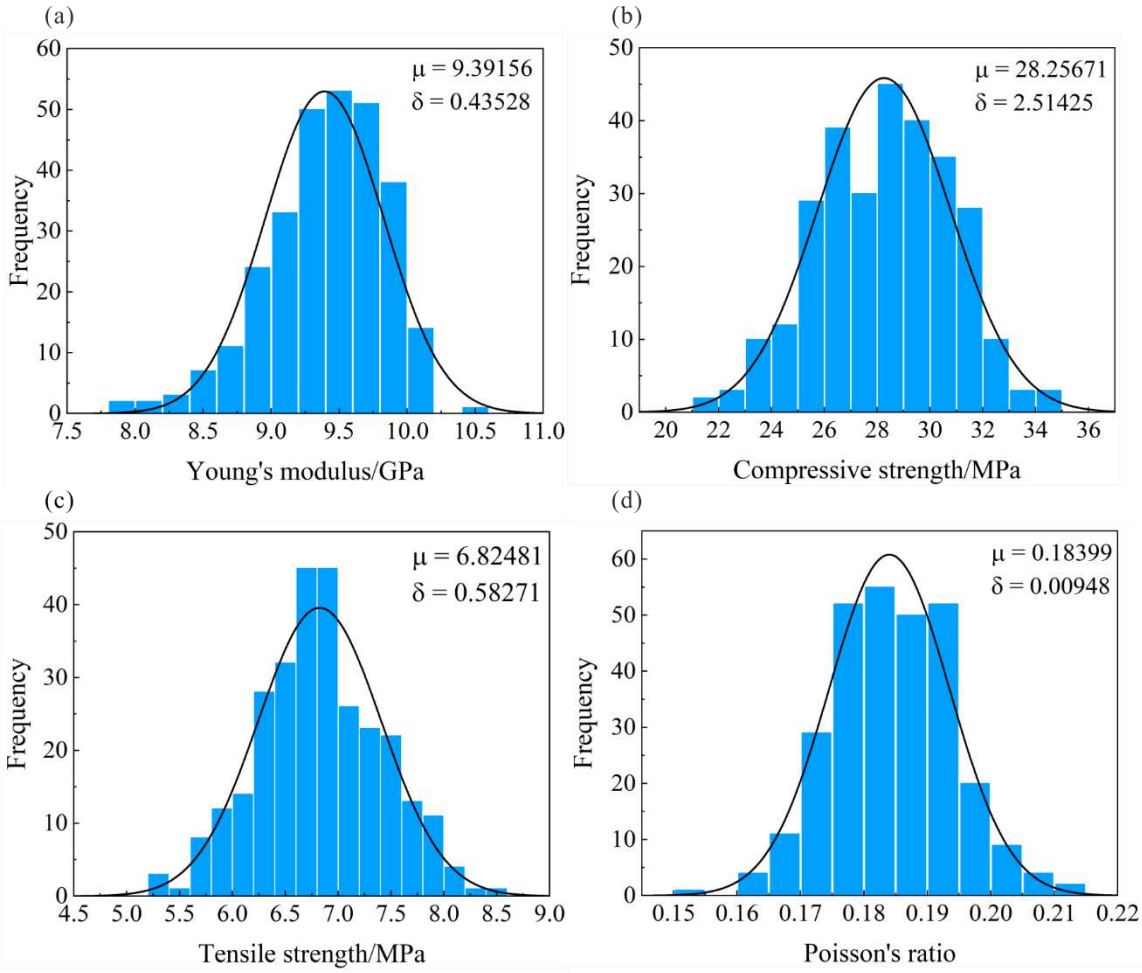

Fig. 3 Histogram of the macroscopic property results with different particle distributions: (a) Young's modulus; (b) compressive strength; (c) tensile strength; (d) Poisson's ratio.

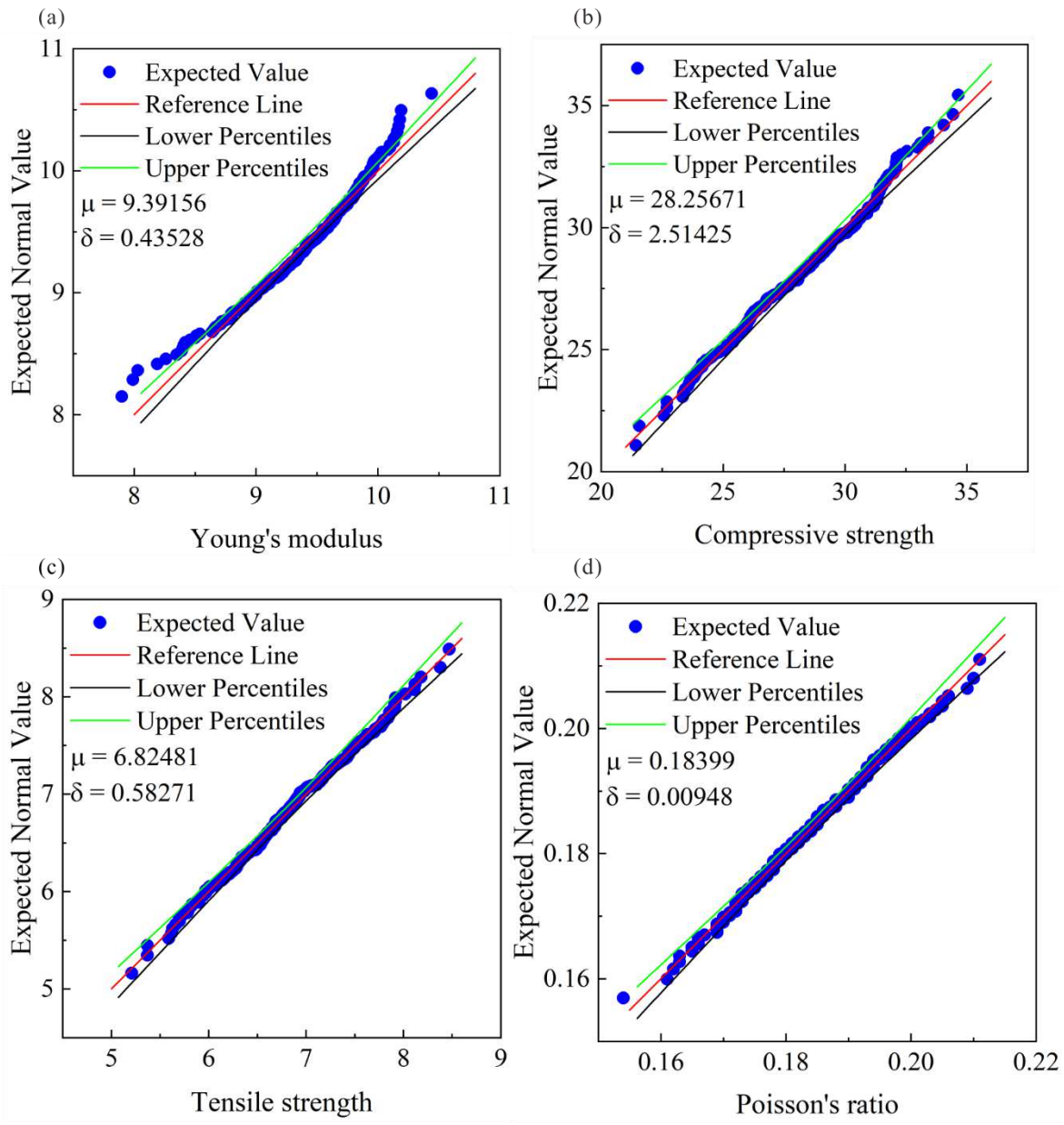

Fig. 4 Q-Q diagram of the macroscopic property results with different particle distributions: (a) Young's modulus; (b) Compressive strength; (c) Tensile strength; (d) Poisson's ratio

To determine the specific distributions for the results of Young's modulus, the raw data that do not follow a standard normal distribution need to be converted. Commonly used conversion methods are the logarithmic transformation, square root transformation and reciprocal transformation (Nishida, 2010), as defined in the following:

$$y = ln\left(K - x\right)$$

9.

$$y = \sqrt{\left|\left(K - x\right)\right|}$$

10.

$$y = \frac{1}{K - x}$$

11.

Where, K is a constant, x and y are the original and transformed data, respectively.

The coefficient K is obtained by letting the skewness of transformed data equal to zero. After trial and error, the logarithmic transformation is used for the Young's modulus data. The coefficient K for Young's modulus 11.384.

Normality tests are performed on the transformed data, and the results are shown in Table 4, Fig. 5 and Fig. 6. The U test values, the significance of LL test and S-W test of the Young's modulus after the transformation meet the standard of normal distributions. Meanwhile, almost all of the data points in the normal Q-Q diagram are within the range corresponding to the confidence level. In summary, the transformed data of Young's modulus follow the normal distribution, and the original data of Young's modulus follows negatively skewed distributions.

Table 4 Results of normality test after data conversion

Items	Young's modulus
Conversion method	logarithmic

Skewness, g_1	0
Skewness Std. Deviation, σ_{g1}	0.143
U test, u_1	0
Kurtosis, g_2	0.018
Kurtosis Std. Deviation, σ_{g2}	0.286
U test, u_2	0.063
LL (P)	0.2
S-W (P)	0.969
Normality (after data conversion)	Yes

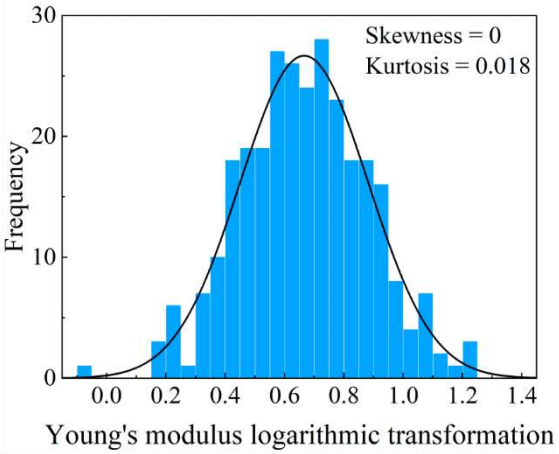

Fig. 5 Histogram of macroscopic property result after Young's modulus data conversion

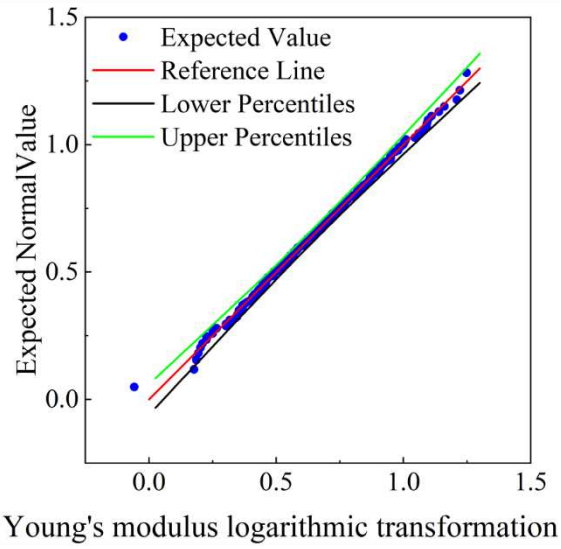

Fig. 6 Q-Q graph of the macroscopic property result after Young's modulus data conversion

3.2 Determination of the minimum sample size for high-precision averages

It has been demonstrated that the randomness of particle distribution has a significant effect on the results of macroscopic mechanical properties of the discrete element model. So in model calibrations, the averages obtained from multiple calculations with different particle distributions should be used, instead of the results from one calculation without considering particle distributions. The approach to determine the number of computations (sample size) is of significant. Apparently, the larger the sample size, the smaller the deviations of averages (Naing, 2003); but in practice, due to the limitation of computing resource, it is impossible to perform infinite calculations to obtain the true averages. Therefore, the correlation between the sample size and the precision of the corresponding average values needs to be studied, then a reasonable calculation number that balances the computing accuracy and efficiency can be determine.

According to the fundamental theory of random sampling, the minimum sample size required to obtain an average for a given precision can be determined according to the total sample variance, allowable error (accuracy) and confidence (Naing, 2003):

$$n_{min} = \frac{Z^2 S^2}{\Delta_{\bar{x}}^2} \tag{12}$$

The standard deviations of the population samples of each item can be found in Table 3. The selection confidence is 95%. The minimum sample size of each macroscopic properties

under different accuracy are calculated According to Eq. 12, and the results are shown in Fig. 7 (a). The results indicate that the minimum sample size becomes larger when the preset error decreases. The fitted curves are also shown in Fig. 7 (a); the minimum sample size for all macroscopic parameters are inversely proportional to the square of error. By comparing the minimum sample size of each item with the same precision, it can be found that the minimum sample size of tensile strength is always the largest. The confidence level also affects the minimum sample size. As Fig. 7(b) shows, at the same precision, the minimum sample size increases with the confidence level.

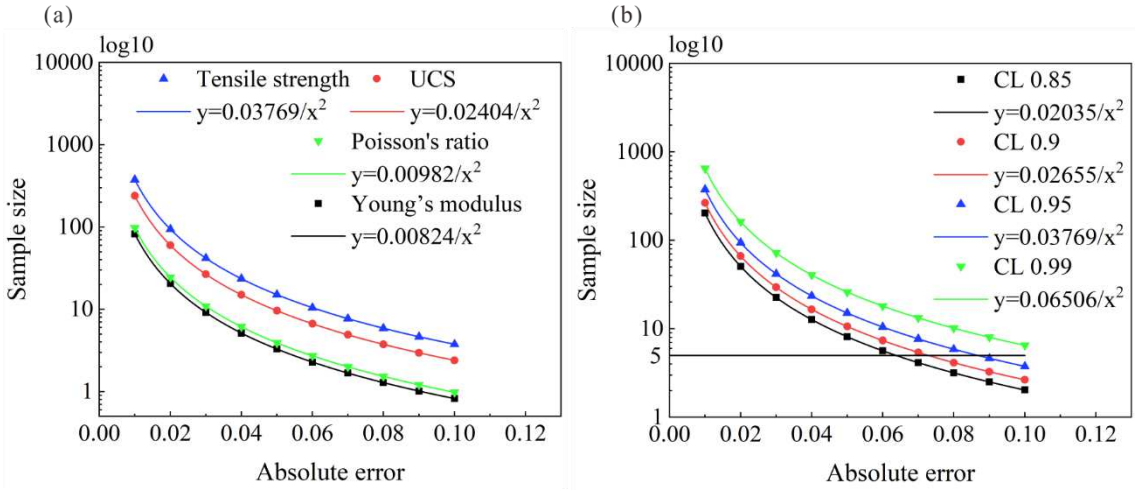

Fig. 7 Determination of the minimum sample size :(a) the minimum sample size of each item varies with the accuracy level when the confidence is 95%; (b) the minimum sample size of tensile strength with given accuracy level under different confidence levels

3.3 Verification of the "three in five tests for the mean" method

The "three in five tests for the mean" method (which is shortened as “three in five” method

in the following) is popular in the investigations involving stochastic problems. In this method, each test will be repeated five times, and the middle three values are adopted to calculate the average. To verify the applicability of the “three in five” method in calculating the averages that used for calibrations, five data points of macroscopic properties are randomly selected from the sample, then the maximum and minimum values are removed and the average are calculated according to the remaining three values. The sampling process is repeated for 20 times, and the corresponding averages are shown in Fig. 8.

All the results (Fig. 8) of Young's modulus, compressive strength, tensile strength and Poisson's ratio show a certain degree of dispersion, but the relative errors of the averages obtained by the “three in five” method are largely smaller ±5%. The maximum error in Fig. 8 is about 7.5%. As shown by Fig. 7 (b), when sample size is five, the relative error of the average is about 8.7% which is larger than that of the average obtained by the “three in five” method where the effects of maximum and minimum are eliminated. In summary, the "three in five" method works well for the problem of calculating the averages that used for calibrations.

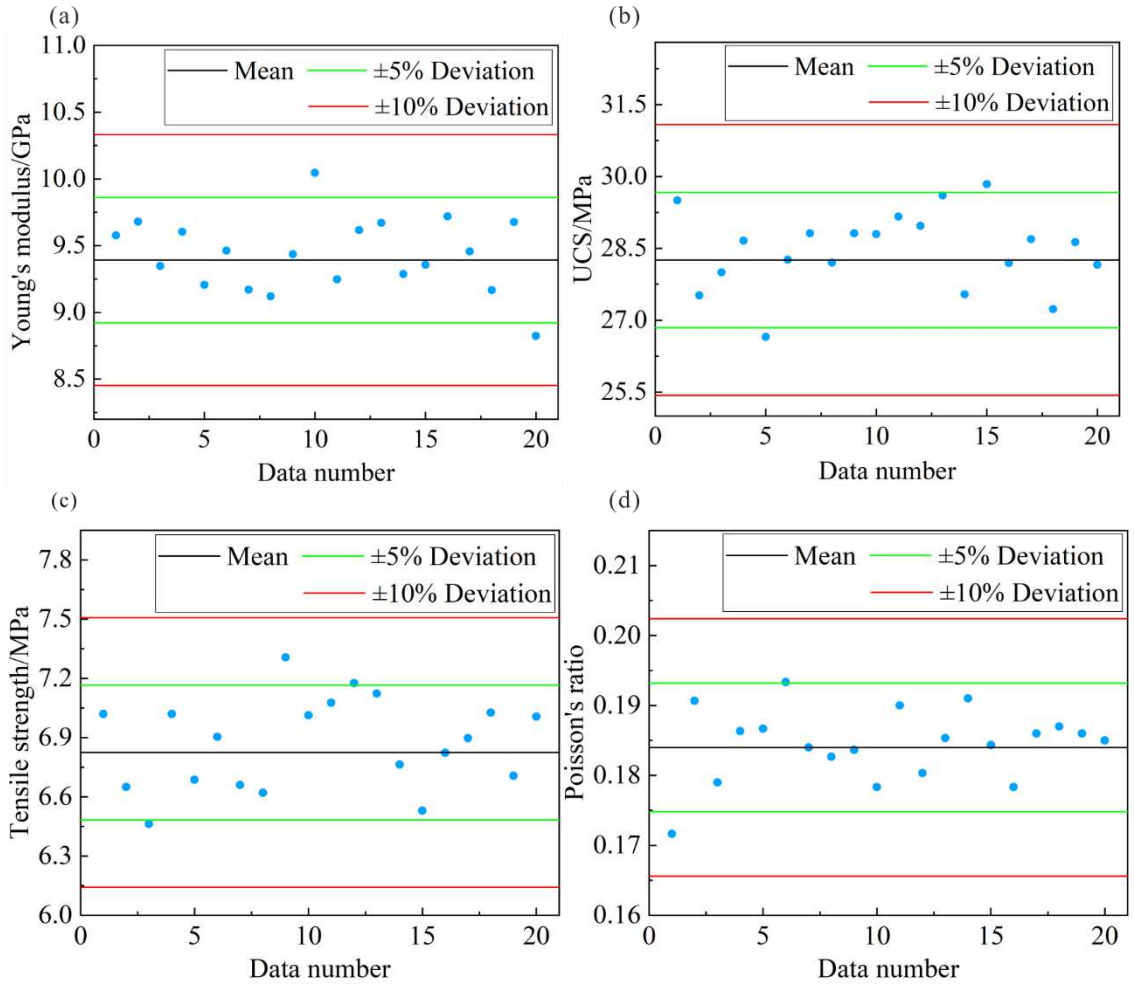

Fig. 8 Error analysis of the averages obtained by the "five choose three" method : (a) Young's modulus; (b) compressive strength; (c) tensile strength; (d) Poisson's ratio.

4 Conclusion

In this paper, the statistical rule of the influence of particle distributions on the macroscopic mechanical property discreteness of the particle flow model is studied. The major conclusions are as follows:

a. The particle distributions have a significant effect on the macroscopic mechanical properties of particle flow model, and the simulation results of compressive strength, tensile

strength and Poisson's ratio with different particle distributions follows normal distributions, while that of Young's modulus follow negative skewness distributions. Therefore, the averages obtained from multiple calculations with different particle distributions should be used for model calibrations, instead of the results from one calculation without considering particle distributions.

b. The minimum sample size required to obtain averages of macroscopic mechanical properties with a given precision level is inversely proportional to the square of precision.

c. The "three in five" method (calculating five times with different particle distributions and calculate the average value after removing the maximum and minimum) is adopted to obtain the averages of macroscopic mechanical properties that used for model calibrations. The deviations of the averages provided by this method is largely within the range of ±5% while the maximum of deviations is not over ±10%, suggesting that the "three in five" method is effective.

Acknowledgement

The authors would like to thank the support from National Natural Science Foundation of China (Grant No.52005419), Key research and development project of Sichuan Province(21ZDYF3658),Major Scientific and Technological Innovation Projects in Chengdu

(2019-YF08-00100-GX)and China postdoctoral science foundation (Grant Number 2019M663898XB). China railway engineering services co. LTD is also acknowledged.

References

. M. M. and . A. P. (2003) 'Type I Error Rate and Power of Three Normality Tests', *Information Technology Journal*, 2(2), pp. 135–139. doi: 10.3923/itj.2003.135.139.

Boutt, D. F. and McPherson, B. J. O. L. (2002) 'Simulation of sedimentary rock deformation: Lab-scale model calibration and parameterization', *Geophysical Research Letters*, 29(4), pp. 13-1-13–4. doi: 10.1029/2001GL013987.

Castro-Filgueira, U. *et al.* (2016) 'Numerical simulation of the stress-strain behavior of intact granite specimens with particle flow code', *ISRM International Symposium - EUROCK 2016*, (August), pp. 421–426. doi: 10.1201/9781315388502-72.

Castro-Filgueira, U. *et al.* (2017) 'Sensitivity Analysis of the Micro-Parameters Used in a PFC Analysis Towards the Mechanical Properties of Rocks', *Procedia Engineering*, 191, pp. 488–495. doi: 10.1016/j.proeng.2017.05.208.

Castro-Filgueira, U., Alejano, L. R. and Ivars, D. M. (2020) 'Particle flow code simulation of intact and fissured granitic rock samples', *Journal of Rock Mechanics and Geotechnical Engineering*, 12(5), pp. 960–974. doi: 10.1016/j.jrmge.2020.01.005.

Cho, N., Martin, C. D. and Sego, D. C. (2007) 'A clumped particle model for rock', *International Journal of Rock Mechanics and Mining Sciences*, 44(7), pp. 997–1010. doi: 10.1016/j.ijrmms.2007.02.002.

Coetzee, C. J. and Els, D. N. J. (2009) 'Calibration of discrete element parameters and the modelling of silo discharge and bucket filling', *Computers and Electronics in Agriculture*, 65(2), pp. 198–212. doi: 10.1016/j.compag.2008.10.002.

Cook, B. K. *et al.* (2004) 'Discrete Element Modeling Applied to Laboratory Simulation of Near-Wellbore Mechanics', *International Journal of Geomechanics*, 4(1), pp. 19–27. doi: 10.1061/(asce)1532-3641(2004)4:1(19).

Cui, J. *et al.* (2017) 'Estimation of the number of specimens required for acquiring reliable rock mechanical parameters in laboratory uniaxial compression tests', *Engineering Geology*, 222, pp. 186–200. doi: 10.1016/j.enggeo.2017.03.023.

Hazzard, J. F., Young, R. P. and Maxwell, S. C. (2000) 'Micromechanical modeling of cracking and failure in brittle rocks', *Journal of Geophysical Research: Solid Earth*, 105(B7), pp. 16683–16697. doi: 10.1029/2000jb900085.

Jing, L. (2003) 'A review of techniques, advances and outstanding issues in numerical modelling for rock mechanics and rock engineering', *International Journal of Rock Mechanics and Mining Sciences*. Elsevier BV, pp. 283–353. doi: 10.1016/S1365-1609(03)00013-3.

Keskin, S. (2006) 'Comparison of Several Univariate Normality Tests Regarding Type I Error Rate and Power of the Test in Simulation based Small Samples', *Power*, 2(5), pp. 296–300.

Lee, C., Park, S. and Jeong, J. (2016) 'Comprehensive comparison of normality tests: Empirical study using many different types of data', *Journal of the Korean Data and Information Science Society*, 27(5), pp. 1399–1412. doi: 10.7465/jkdi.2016.27.5.1399.

Massey, F. J. (1951) 'The Kolmogorov-Smirnov Test for Goodness of Fit', *Journal of the*

American Statistical Association, 46(253), pp. 68–78. doi: 10.1080/01621459.1951.10500769.

McDowell, G. R. *et al.* (2006) 'Discrete element modelling of geogrid-reinforced aggregates', *Proceedings of the Institution of Civil Engineers: Geotechnical Engineering*, 159(1), pp. 35–48. doi: 10.1680/geng.2006.159.1.35.

Mehranpour, M. H. and Kulatilake, P. H. S. W. (2017) 'Improvements for the smooth joint contact model of the particle flow code and its applications', *Computers and Geotechnics*, 87, pp. 163–177. doi: 10.1016/j.compgeo.2017.02.012.

Mohd Razali, N. and Bee Wah, Y. (2011) 'Power comparisons of Shapiro-Wilk, Kolmogorov-Smirnov, Lilliefors and Anderson-Darling tests', *Journal of Statistical Modeling and Analytics*, 2(1), pp. 21–33.

Moon, T. and Oh, J. (2012) 'A study of optimal rock-cutting conditions for hard rock TBM using the discrete element method', *Rock Mechanics and Rock Engineering*, 45(5), pp. 837–849. doi: 10.1007/s00603-011-0180-3.

Naing, N. N. (2003) 'Determination of sample size', *Malaysian Journal of Medical Sciences*, 10(2), pp. 84–86.

Nishida, T. (2010) '[Data transformation and normalization].', *Rinsho byori. The Japanese journal of clinical pathology*, 58(10), pp. 990–997.

Onate, E. and Rojek, J. (2004) 'Combination of discrete element and finite element methods for dynamic analysis of geomechanics problems', *Computer Methods in Applied Mechanics and Engineering*, 193(27–29), pp. 3087–3128. doi: 10.1016/j.cma.2003.12.056.

Öztuna, D., Elhan, A. H. and Tüccar, E. (2006) 'Investigation of four different normality tests

391 in terms of type 1 error rate and power under different distributions', *Turkish Journal of*
392 *Medical Sciences*, 36(3), pp. 171–176.
393 Potyondy, D. O. and Cundall, P. A. (2004) 'A bonded-particle model for rock', *International*
394 *Journal of Rock Mechanics and Mining Sciences*, 41(8 SPEC.ISS.), pp. 1329–1364. doi:
395 10.1016/j.ijrmms.2004.09.011.
396 Qin, S. *et al.* (2013) 'Numerical studies of cutting water saturated sand by discrete element
397 method', in *Applied Mechanics and Materials*. doi: 10.4028/www.scientific.net/AMM.256-
398 259.306.
399 Ruffolo, R. M. and Shakoor, A. (2009) 'Variability of unconfined compressive strength in
400 relation to number of test samples', *Engineering Geology*, 108(1–2), pp. 16–23. doi:
401 10.1016/j.enggeo.2009.05.011.
402 Schöpfer, M. P. J. *et al.* (2009) 'The impact of porosity and crack density on the elasticity,
403 strength and friction of cohesive granular materials: Insights from DEM modelling',
404 *International Journal of Rock Mechanics and Mining Sciences*, 46(2), pp. 250–261. doi:
405 10.1016/j.ijrmms.2008.03.009.
406 Shapiro, S. S. and Wilk, M. B. (1965) 'An Analysis of Variance Test for Normality (Complete
407 Samples)', *Biometrika*, p. 591. doi: 10.2307/2333709.
408 Shapiro, S. S. and Wilk, M. B. (1972) 'An Analysis of Variance Test for the Exponential
409 Distribution (Complete Samples)', *Technometrics*, 14(2), pp. 355–370. doi:
410 10.1080/00401706.1972.10488921.
411 Shi, C. *et al.* (2019) 'Calibration of micro-scaled mechanical parameters of granite based on a

412 bonded-particle model with 2D particle flow code', *Granular Matter*, 21(2). doi:
413 10.1007/s10035-019-0889-3.
414 Society, R. S. (2019) 'Remark AS R94 : A Remark on Algorithm AS 181 : The W-test for
415 Normality Author (s): Patrick Royston Source : Journal of the Royal Statistical Society . Series
416 C (Applied Statistics), Vol . 44 , No . 4 Published by : Wiley for the Royal Statistical Soc',
417 44(4), pp. 547–551.
418 Tian, W. L. *et al.* (2020) 'Mechanical Behavior of Granite with Different Grain Sizes After
419 High-Temperature Treatment by Particle Flow Simulation', *Rock Mechanics and Rock*
420 *Engineering*, 53(4), pp. 1791–1807. doi: 10.1007/s00603-019-02005-1.
421 Trust, B. (2016) 'Biometrika Trust Tests for Departure from Normality . Empirical Results for
422 the Distributions of b2 and √ b Author (s): Ralph D ' Agostino and E . S . Pearson Published
423 by : Oxford University Press on behalf of Biometrika Trust Stable URL : http://www.j', 60(3),
424 pp. 613–622.
425 Wang, R. (1981) 'Fundamentals of rock mechanics', *Earth-Science Reviews*, 17(3), p. 302. doi:
426 10.1016/0012-8252(81)90052-0.
427 Wang, Y. and Tonon, F. (2010) 'Calibration of a discrete element model for intact rock up to
428 its peak strength', *International Journal for Numerical and Analytical Methods in*
429 *Geomechanics*, 34(5), pp. 447–469. doi: 10.1002/nag.811.
430 Xia, L. and Zeng, Y. (2018) 'Parametric study of smooth joint parameters on the mechanical
431 behavior of transversely isotropic rocks and research on calibration method', *Computers and*
432 *Geotechnics*, 98(January), pp. 1–7. doi: 10.1016/j.compgeo.2018.01.012.

Xie, L. *et al.* (2020) 'Numerical simulation of uniaxial compression tests on layered rock specimens using the discrete element method', *Computational Particle Mechanics*, 7(4), pp. 753–762. doi: 10.1007/s40571-019-00307-3.

Yamaguchi, U. (1970) 'THE NUMBER DETERMINE TEST-PIECES STRENGTH REQUIRED OF TO THE University of Tokyo , Tokyo , Japan Abstract--Studies to determine the number of test-pieces required to test the strength of rock are reported . The number of test-pieces reqmred is quantitativ', 7, pp. 209–227.

Yap, B. W. and Sim, C. H. (2011) 'Comparisons of various types of normality tests', *Journal of Statistical Computation and Simulation*, 81(12), pp. 2141–2155. doi: 10.1080/00949655.2010.520163.

Yoon, J. (2007) 'Application of experimental design and optimization to PFC model calibration in uniaxial compression simulation', *International Journal of Rock Mechanics and Mining Sciences*, 44(6), pp. 871–889. doi: 10.1016/j.ijrmms.2007.01.004.

Zhang, Q. Q. *et al.* (2015) 'Numerical simulation of rock cutting in different cutting mode using the discrete element method', *Journal of GeoEngineering*, 10(2), pp. 35–43. doi: 10.6310/jog.2015.10(2).1.

Zhao, H. *et al.* (2019) 'Hierarchical Modeling Method for DEM Simulation and Its Application in Soil–Pile–Cap Interaction and Impact Case', *International Journal of Geomechanics*, 19(7), p. 04019076. doi: 10.1061/(asce)gm.1943-5622.0001467.

Figure captions

Fig. 1 Particle flow models for simulating uniaxial tests and typical results: (a) model for uniaxial compression tests; (b) crack distribution after uniaxial compression tests; (c) model for uniaxial tensile tests; (d) crack distribution after uniaxial tensile tests

Fig. 2 Stress-strain response: (a) uniaxial compression tests; (b) uniaxial tensile tests

Fig. 3 Histogram of the macroscopic property results with different particle distributions: (a) Young's modulus; (b) compressive strength; (c) tensile strength; (d) Poisson's ratio.

Fig. 4 Q-Q diagram of the macroscopic property results with different particle distributions: (a) Young's modulus; (b) Compressive strength; (c) Tensile strength; (d) Poisson's ratio

Fig. 5 Histogram of macroscopic property result after Young's modulus data conversion

Fig. 6 Q-Q graph of the macroscopic property result after Young's modulus data conversion

Fig. 7 Determination of the minimum sample size :(a) the minimum sample size of each item varies with the accuracy level when the confidence is 95%; (b) the minimum sample size of tensile strength with given accuracy level under different confidence levels

Fig. 8 Error analysis of the averages obtained by the "five choose three" method : (a) Young's modulus; (b) compressive strength; (c) tensile strength; (d) Poisson's ratio.

Figures

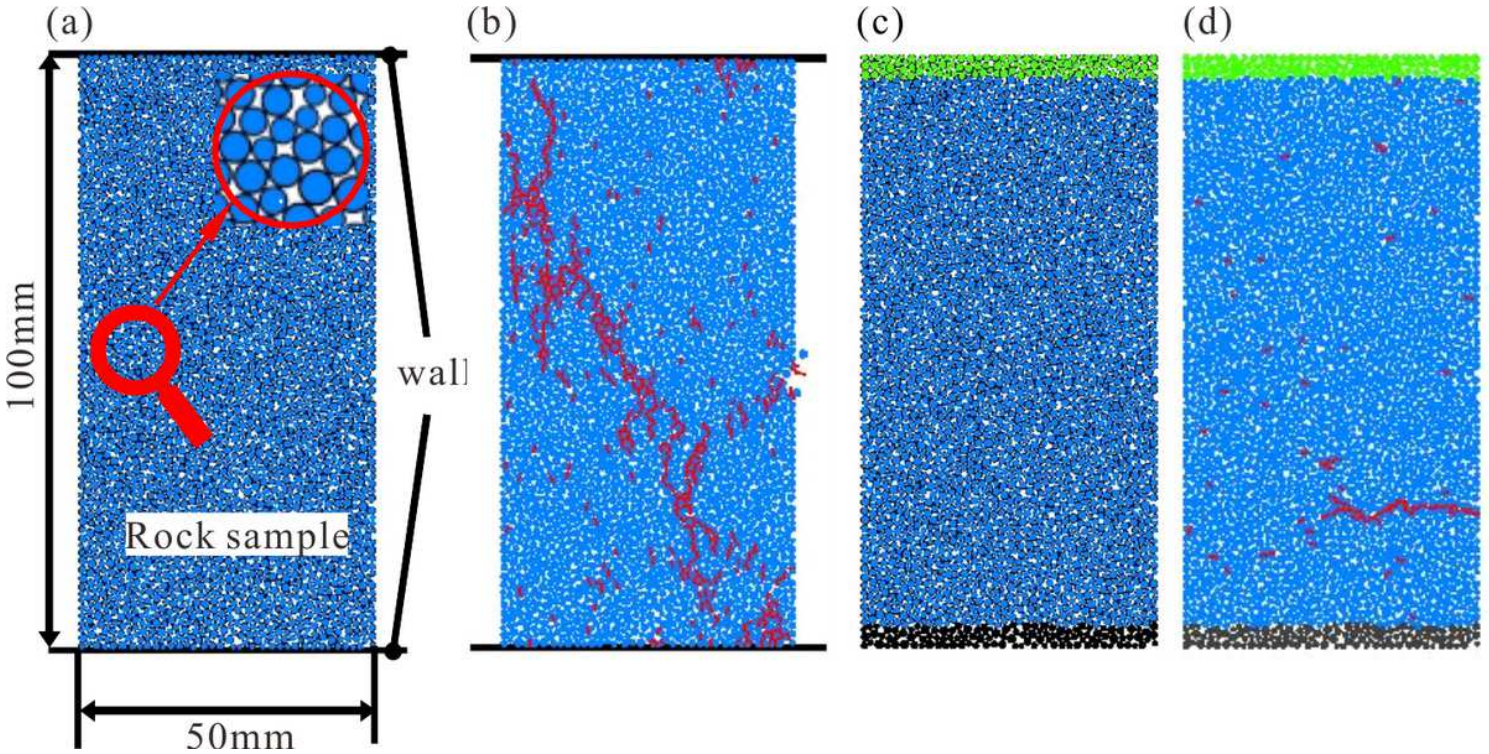

Figure 1

Particle flow models for simulating uniaxial tests and typical results: (a) model for uniaxial compression tests; (b) crack distribution after uniaxial compression tests; (c) model for uniaxial tensile tests; (d) crack distribution after uniaxial tensile tests

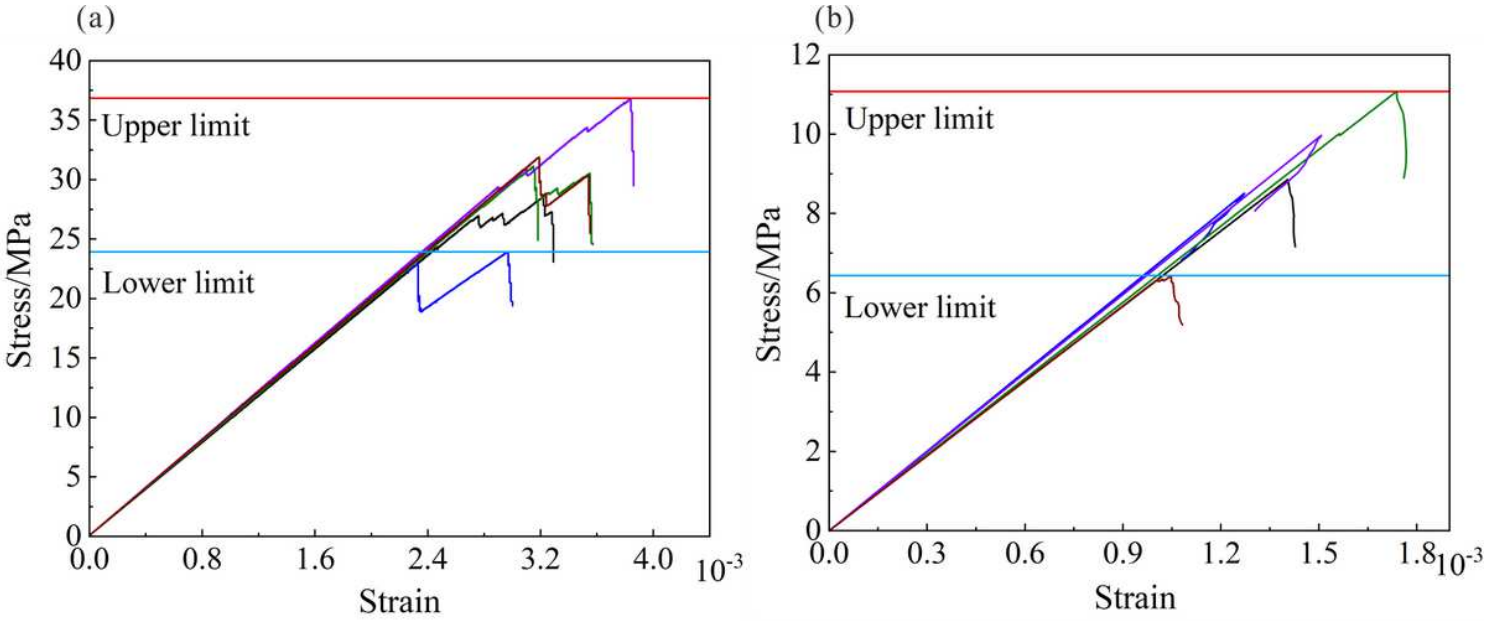

Figure 2

Stress-strain response: (a) uniaxial compression tests; (b) uniaxial tensile tests

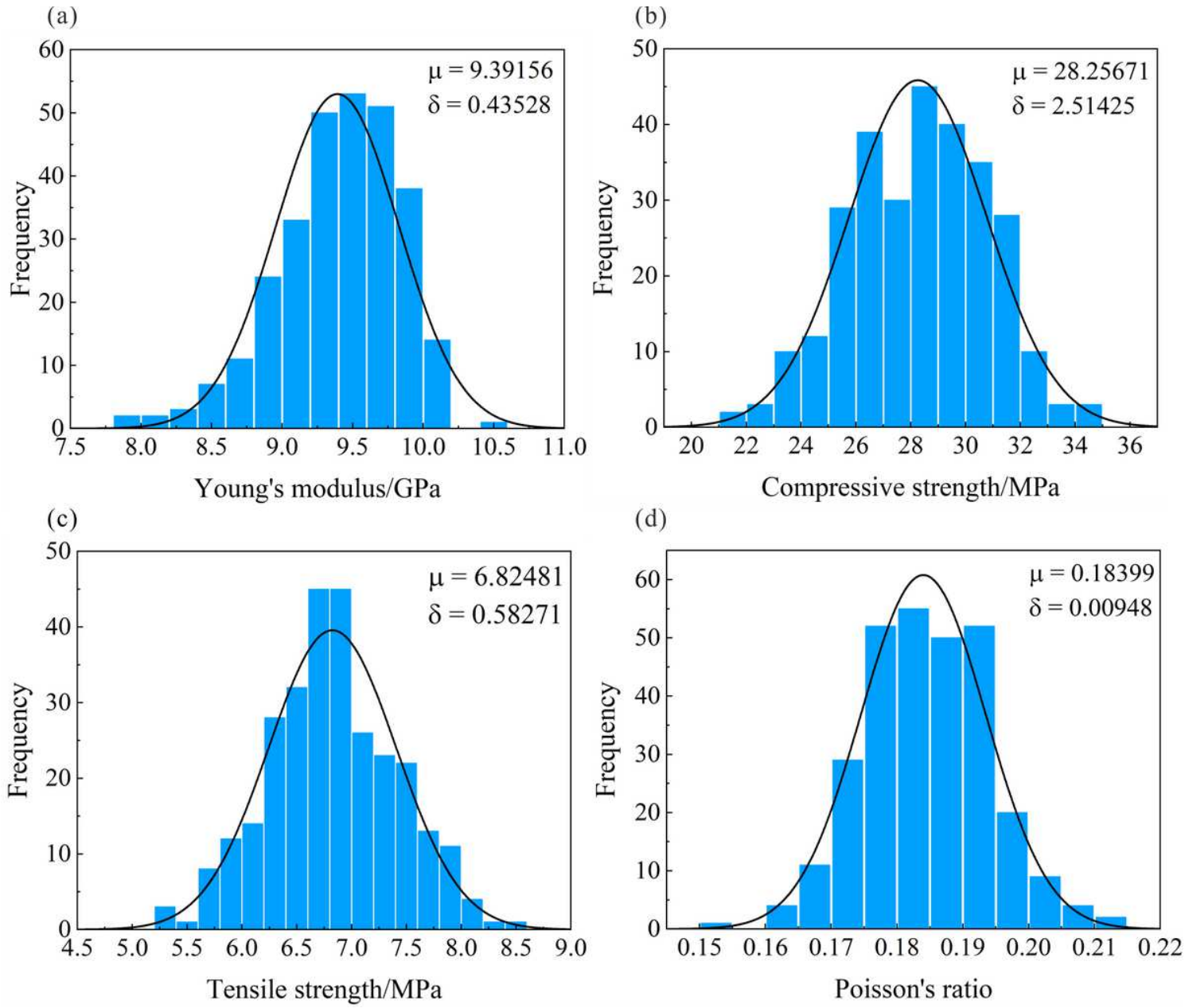

Figure 3

Histogram of the macroscopic property results with different particle distributions: (a) Young's modulus; (b) compressive strength; (c) tensile strength; (d) Poisson's ratio.

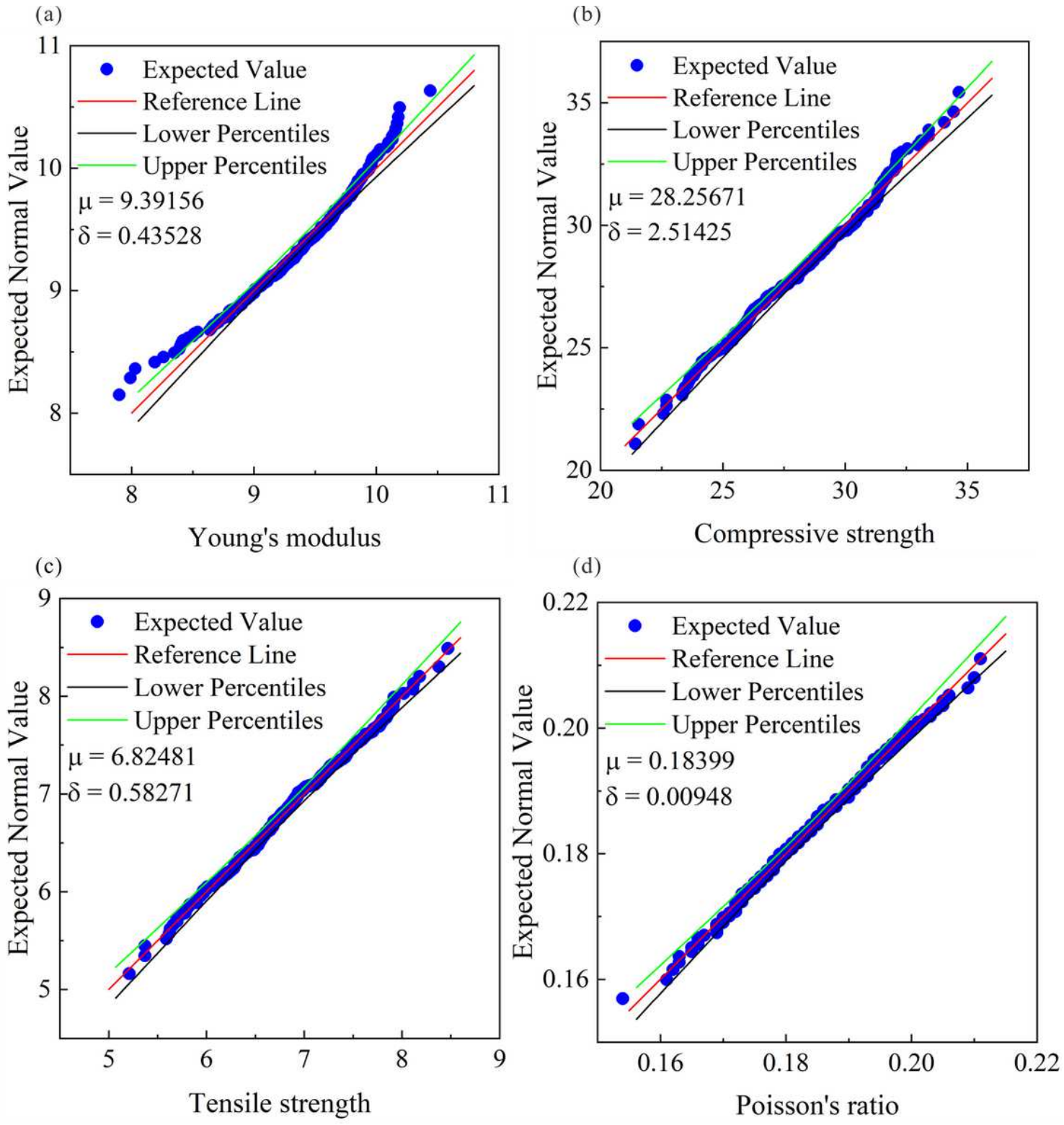

Figure 4

Q-Q diagram of the macroscopic property results with different particle distributions: (a) Young's modulus; (b) Compressive strength; (c) Tensile strength; (d) Poisson's ratio

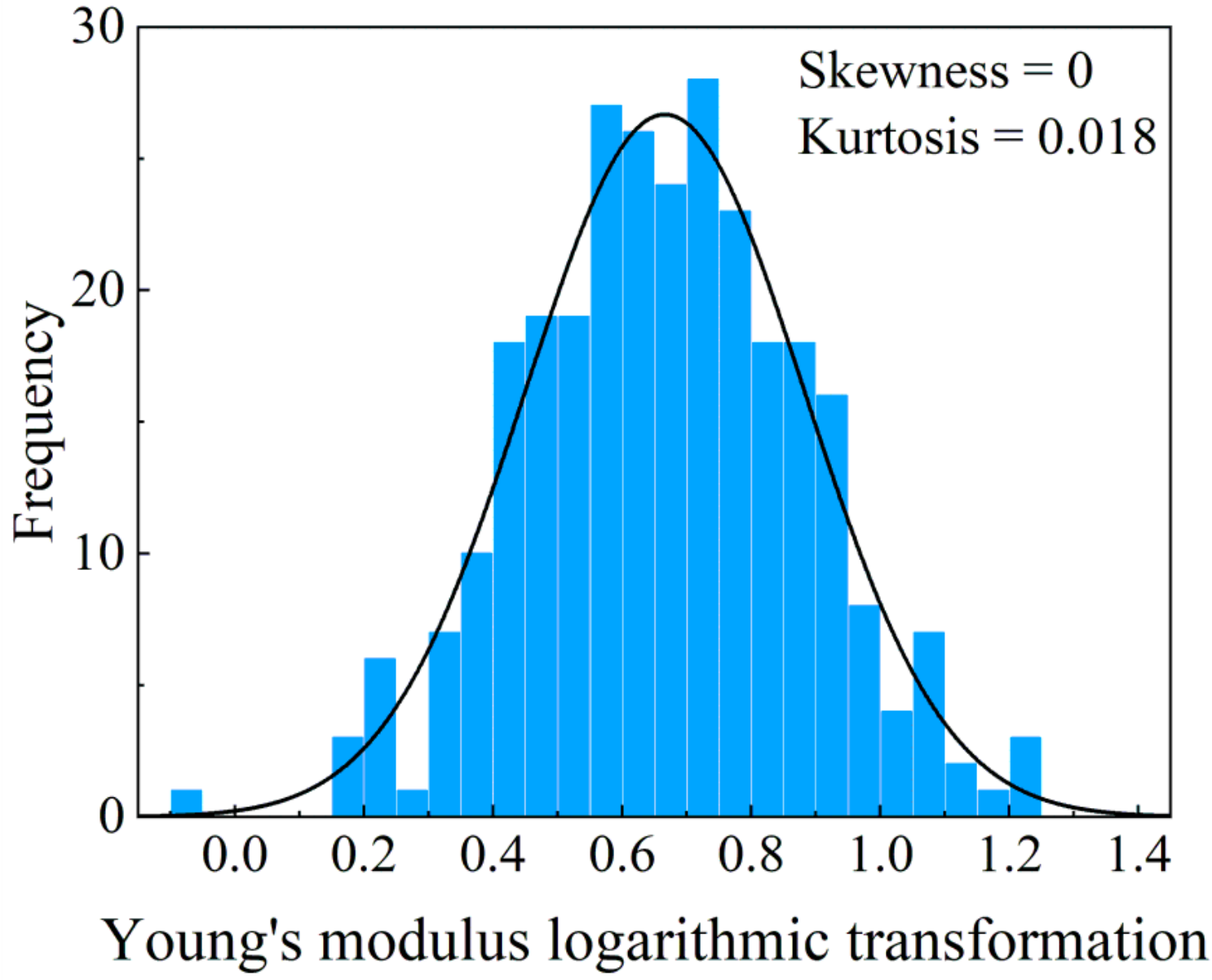

Figure 5

Histogram of macroscopic property result after Young's modulus data conversion

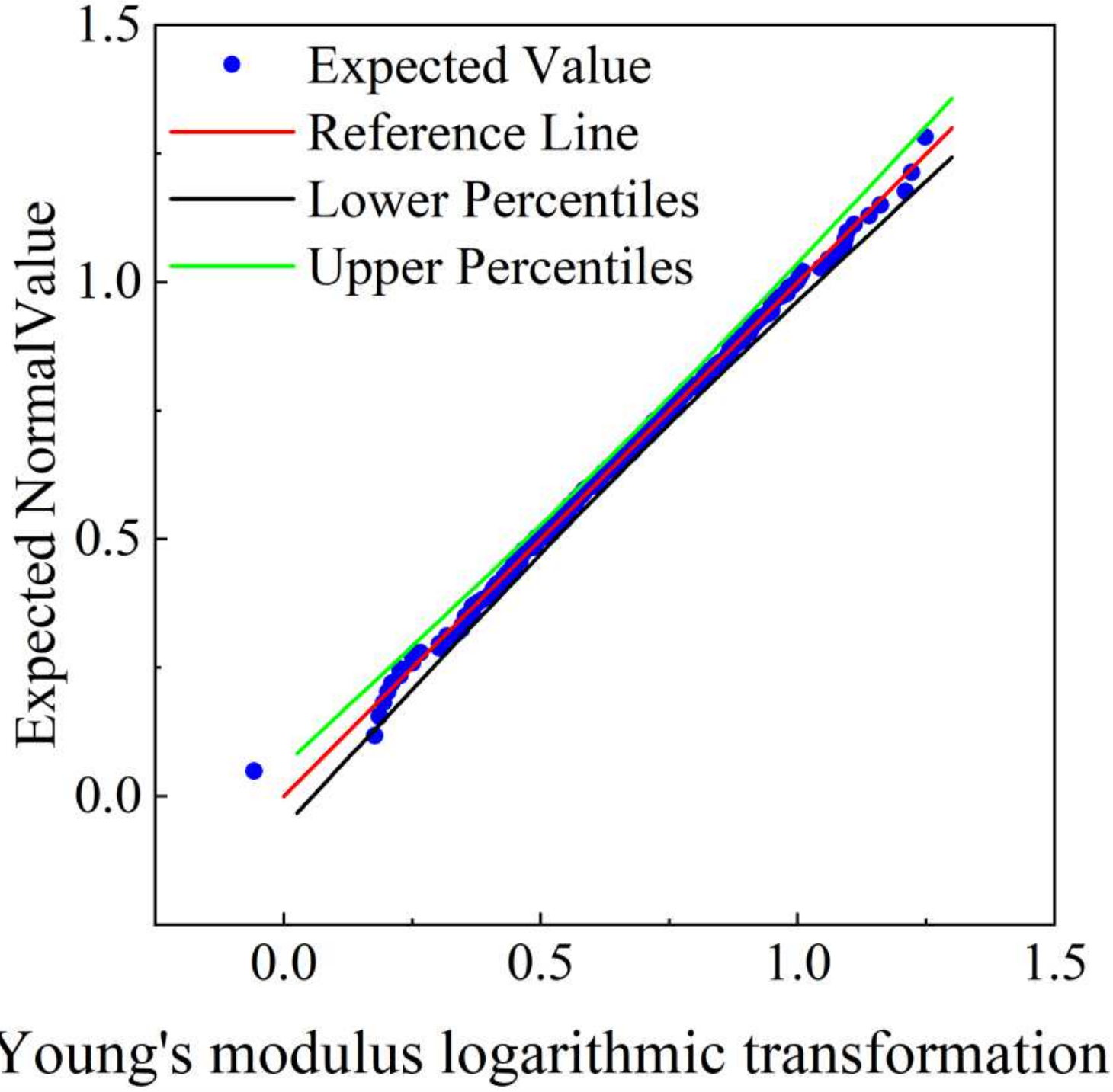

Figure 6

Q-Q graph of the macroscopic property result after Young's modulus data conversion

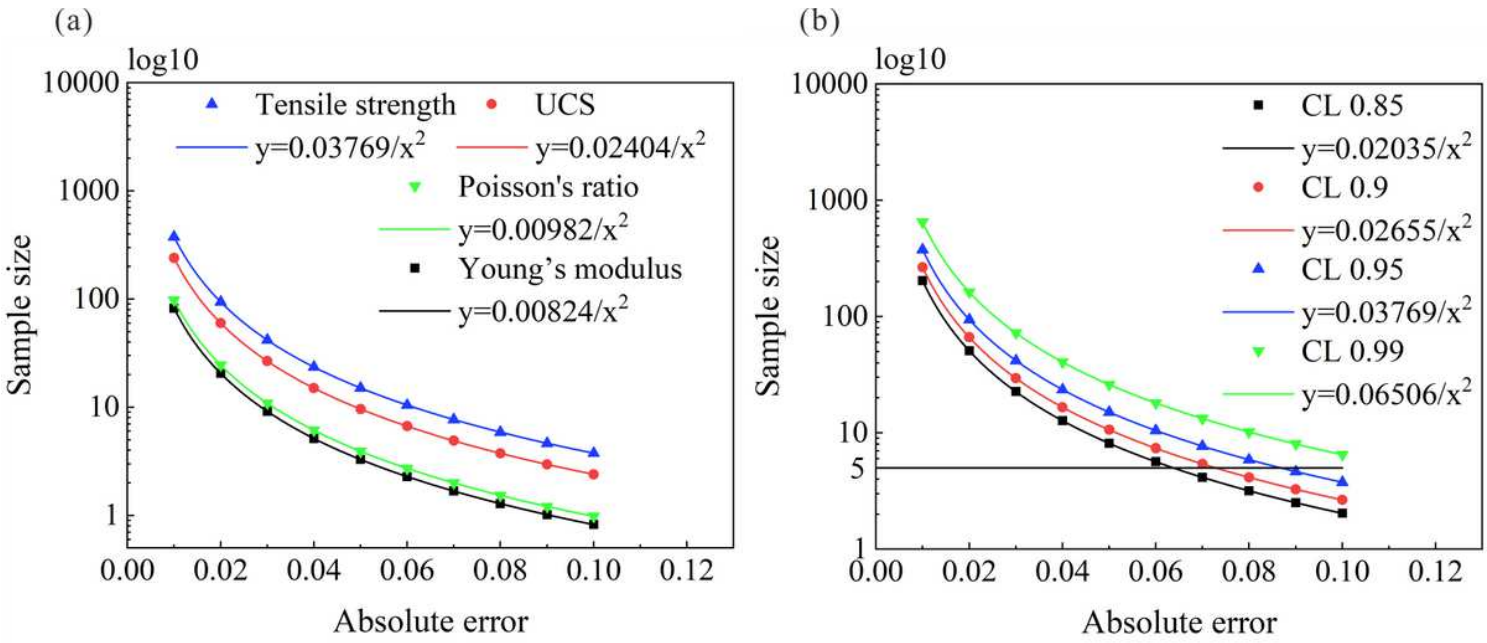

Figure 7

Determination of the minimum sample size :(a) the minimum sample size of each item varies with the accuracy level when the confidence is 95%; (b) the minimum sample size of tensile strength with given accuracy level under different confidence levels

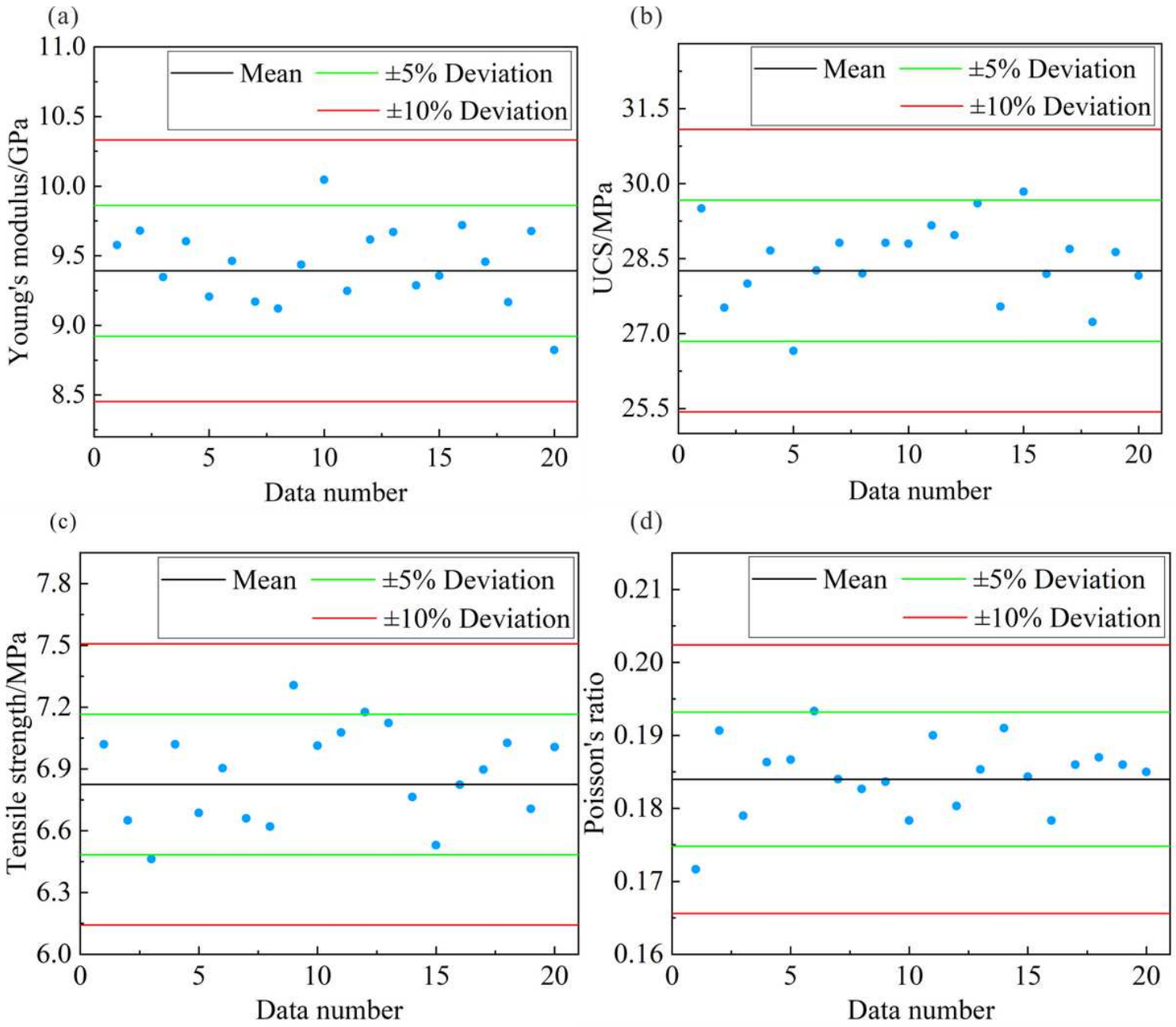

Figure 8

Error analysis of the averages obtained by the "five choose three" method : (a) Young's modulus; (b) compressive strength; (c) tensile strength; (d) Poisson's ratio.